

Analysis of the Particle Resuspension Factor Shortly After a Surface Release

Submitted by Holden Snyder

Advised by David Medich



Department of Physics, Worcester Polytechnic Institute
April 28, 2022

This report represents the work of one or more WPI undergraduate students submitted to the faculty as evidence of completion of a degree requirements. WPI routinely publishes these reports on the web without editorial or peer review.

Abstract

The current empirical resuspension factor is based on the work of Maxwell and Anspaugh (2011). This resuspension factor was determined by fitting a double exponential to the collective data of over sixty different studies. The majority of these studies were airborne release events, and very few were surface releases. Further, most of these studies took data points on the order of weeks or months, not days. This has led to an overestimation of the resuspension factor in the early release phase. This is especially true in the case of a surface release, where predicted values are often four orders of magnitude greater than measured values. This report seeks to show the discrepancy between the predicted resuspension factor, and the measured resuspension factor at small times for a surface release.

Acknowledgements

I would like to thank David Medich for his advice and for allowing me the use of his lab. I would also like to thank Shaun Marshall for his valuable advice and information on the resuspension factor.

Thank you to Kiran Tremblay, Isaac Peturiziello, and Kim Nguyen for proofreading this report.

Thank you to Nicole Dombrowski, Aaron Demers, and Lauren Dana for their assistance with setting up, cleaning, and maintaining the resuspension chambers.

This would not have been possible without all of you.

Contents

1	Introduction	1
2	Background	1
2.1	Health Risks of Ionizing Radiation	1
2.1.1	Absorbed and Equivalent Dose	1
2.1.2	Stochastic and Deterministic Risk	3
2.2	Particle Release	5
2.3	The Resuspension Factor	7
2.4	Detection of Radionuclides	9
2.4.1	Neutron Activation Analysis	9
2.4.2	Minimum detectable mass	12
2.4.3	Minimum Detectable Resuspension Factor	15
3	Methods	16
3.1	Materials	16
3.1.1	Suspending Material	16
3.1.2	Air Sampling	16
3.1.3	Resuspension chamber	17
3.1.4	Neutron Activation Analysis	17
3.2	Experiment setup	18
3.3	Experiment Procedure	18
3.3.1	Collecting Samples	18
3.3.2	Neutron Activation Analysis	19
3.3.3	Calculation of the Resuspension Factor	22

4	Results	24
5	Analysis	27
5.1	Evaluation of Measured Resuspension Factor	27
5.2	Evaluation of Predicted Resuspension Factor	28
6	Conclusion	30
	References	32

1 Introduction

The resuspension factor is a measure of the relative activity of a radionuclide in the air compared to the surface beneath it. The most influential study into the resuspension factor is the meta-analysis by Maxwell and Anspaugh (2011), which established the resuspension model that is now widely used. While this model is largely accurate at large times ($t > 2$ weeks), this model gives resuspension factor estimates that are more than one hundred times larger than measured for surface releases at small times after deposition. The resuspension factor at large times is well studied, but these small times after deposition do not have nearly the same attention. The variables that affect the resuspension factor such as deposition surface, wind speed, temperature, etc. are similarly unstudied. Following the experimental model established by Marshall (2021), these factors in small time frames are the subject of this report. Specifically, this report seeks to test the Maxwell and Anspaugh model at small times after release in the event of a surface release.

2 Background

2.1 Health Risks of Ionizing Radiation

2.1.1 Absorbed and Equivalent Dose

There are several units of measurement for the exposure of a biological system to ionizing radiation. The most common methods of measuring this quantity are the absorbed dose and equivalent dose. Absorbed dose is the amount of energy deposited

in a body per unit mass. Absorbed dose is measured in units of either rads, or the SI unit Grays (Gy). In SI base units, absorbed dose is measured in J Kg^{-1} . Absorbed dose is used as a measure of the risk to a person's health. However, absorbed dose does not take into account the relative biologic effect of different types of radiation. All radiations are treated the same, and only the energy is taken into account (NRC, 2020).

Equivalent dose is the absorbed dose multiplied by a quality factor, based on the type of ionizing radiation the body is exposed to. The idea behind the equivalent dose is that certain types of ionizing radiation have the potential to do more damage to cells than other. Heavy charged particles are more likely to interact and to cause breaks in the strands of a cell's DNA, and thus have a higher equivalent dose than light charged particles or photons.

Type of radiation	Quality factor	Absorbed dose equal to a unit dose equivalent ^a
	(Q)	
X-, gamma, or beta radiation	1	1
Alpha particles, multiple-charged particles, fission fragments and heavy particles of unknown charge	20	0.05
Neutrons of unknown energy	10	0.1
High-energy protons	10	0.1

Figure 1: Table of quality factors taken from 10 CFR 20.1004 from the Nuclear Regulatory Commission

1 Rem (equivalent dose) is equivalent to 1 Rad (absorbed dose) times the quality factor. 1 Sievert (equivalent dose) corresponds to 1 Gray (absorbed dose) times a quality factor. Equivalent dose is used in the measurement of the stochastic risk of radiation to the whole body.

2.1.2 Stochastic and Deterministic Risk

According to the Nuclear Regulatory Commission (NRC), ionizing radiation is considered to be any radiation or particle “capable of producing ions.” This includes high energy (>34 eV) photons and other particles like neutrons, betas, alphas, and more. The ions produced from these high energy particles can interrupt the bonds made in living cells and cause changes in the body. High doses of radiation can lead to severe skin or tissue damage, cancer, and acute radiation syndrome (CDC, 2021). This damage can be split into two types of risk: stochastic (random) risk, and deterministic (definite) risk.

Deterministic risk is when a specific dose of radiation, known as the threshold dose, is directly related to a known symptom. Doses in excess of this dose will always show this effect, but below this dose no effect will be observed. Doses above the threshold dose will also increase the severity of the effect. Deterministic risk is most often shown as acute radiation syndrome (ARS), but other symptoms such as skin burns can occur at high doses. ARS, according to the CDC, typically shows symptoms at doses of 70 Rem or more. The radiation dose must also be absorbed in a short amount of time. Due to their relatively low dose rate, ingested radioactive material typically does not cause ARS (CDC, 2021).

Stochastic risk is primarily the increased likelihood of developing cancer due to ionizing radiation. High energy photons or charged particles can impart energy on atomic electrons in a cell’s DNA. This damages the DNA of the cell and either kills the cell, or forces the cell to attempt to repair the DNA. If the cell repairs the DNA incorrectly, this can cause genetic mutations that can lead to cancer after many mitotic

cycles.

Stochastic risk does not have a clean limit for what is typically dangerous like ARS due to its dependence on random chance. It has been conservatively estimated that 1 Rem corresponds to an additional lifetime cancer risk of 0.04% (ICRP, 1990). This risk follows a conservative linear model, so 10 Rem would correspond to an additional risk of .4%. The NRC has set acceptable dose limits for both radiological workers and the general public. These limits are detailed in federal code 10 CFR 20: Standards for Protection Against Radiation. The general public is allowed to receive 100 mRem to their whole body each year. Radiological workers are allowed to receive 5 Rem (.05Sv) to their whole body each year. Additionally, since the absorbed dose of each radiological worker is tracked, they are allowed only 25 Rem in their lifetime (NRC, 2020). The limits set for individual parts of the body like the hands or lens of the eye are different, and usually higher. These limits are often based on deterministic risk, while the whole body limits are based on stochastic risk.

There are also limits to the amount of radioactive material that can be absorbed or ingested by a worker each year. This is defined as the annual limit on intake (ALI) of an isotope. The ALI is the activity of an isotope that, if ingested, would result in an equivalent dose of 5 Rem (NRC, 2020). Ingesting or inhaling a radioactive isotope gives a significantly higher dose per unit mass than a surface deposited source. For example, the ALI of Thallium 201, a randomly selected isotope listed by the NRC, is 2000 μCi . Thus, ingesting 2000 μCi of Tl-201 will typically result in an absorbed dose of about 5 Rem. This same activity of Tl-201, assuming it is a point source 50cm away for a 24 hours, will give an absorbed dose of 1.7 Rem. This is a simple calculation meant to show that the absorbed dose from an inhaled isotope is

significantly higher than the equivalent reasonable exposure to a ground deposited isotope. This is especially true for isotopes that emit heavy charged particles like alphas. Alpha particles are easily blocked by the thin layer of dead skin on people's bodies. Many alphas are caught by this layer of dead skin and cause much less damage to cells when the alpha emitter is outside the body. Ingested alpha particles have access to cells without any protective barrier however, and can cause high damage to cells. For that reason, tracking the ingestion of alpha emitting nuclides is even more critical than other nuclides, and their ALIs are much lower than other nuclides.

2.2 Particle Release

Radioactive particles can be released into the environment by nuclear weapons, reactor meltdowns, dirty bombs, or containment breaches. These radioactive particles then deposit onto surfaces or remain into air. These are examples of airborne releases. Airborne releases are the most common method of release, and are more well studied than surface releases. Initial suspension of particulates in an airborne release can be modeled with a plume equation. There exist several different types of plume equations, depending on the conditions in the release area. Shown below is a Gaussian plume, the most simplistic type of plume equation:

$$X(x, y) = \frac{Q}{\pi\sigma_y\sigma_z\bar{u}} * e^{-\left(\frac{h^2}{2\sigma_z^2} + \frac{y^2}{2\sigma_y^2}\right)} \quad (1)$$

Where Q is the source strength, σ_y and σ_z are the crosswind and vertical plume standard deviations, \bar{u} is the mean wind speed, and h is the effective stack height, and x and y are the downwind and crosswind distances. This plume equations gives a model of initial suspension for particulate concentration downwind from a release

source.

Gaussian Plume model

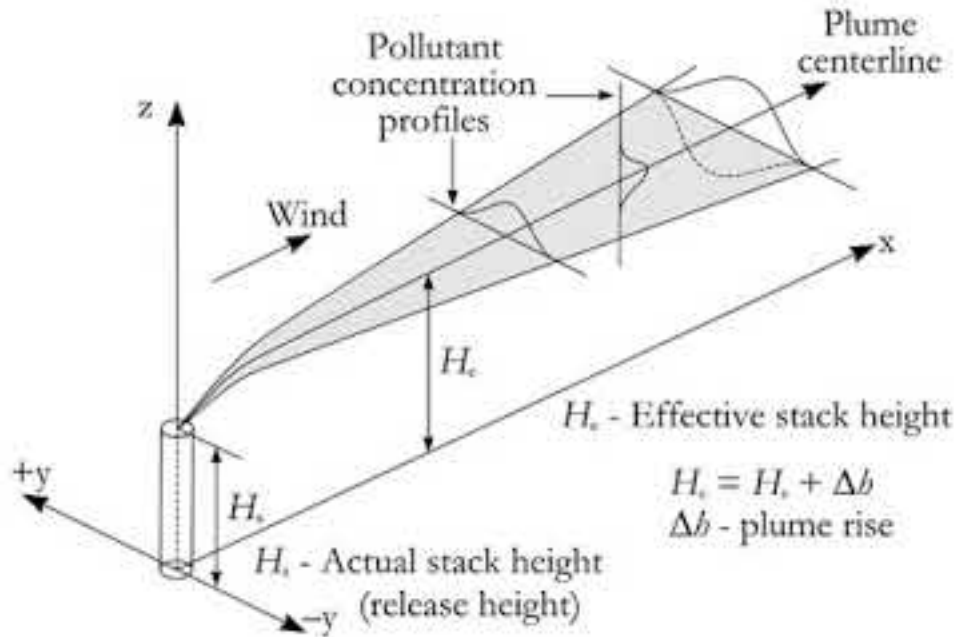


Figure 2: Diagram of a Gaussian plume, where wind carries particulates over and area where they can then deposit.

After the initial suspension, particles will settle onto the ground. These deposited particles can begin to re-suspend as more time passes after the initial release. However, the rate of resuspension from a surface has been a sparsely measured quantity.

A surface release event can also occur when a steady-state contaminated zone is

perturbed, or when precipitation carries radio-particulates to a location and then evaporates. In the case of both a surface release and an airborne release, deposited particles can resuspend into the air by anthropological disturbances (Langham 1971), electrostatic resuspension (Marshall, 2021), wind, or a multitude of other factors. Resuspension, especially in the context of radio-particulates, has been very sparsely covered without a corresponding initial suspension.

2.3 The Resuspension Factor

The resuspension factor is a quantity that directly relates the internal absorbed dose of an individual to the contamination of the area. Resuspending influences are highly dependent on environmental factors such as aerosol size distribution (Karlsson et al. 1996), temperature and pressure of the area (Xu et al., 2016), humidity (Kim et al. 2016), weather and vegetation (Dreicer et al. 1984), lateral wind speed (Harris and Davidson, 2008), and anthropological disturbances (Langham, 1971). The resuspension factor is therefore a site-specific measurement. However, general models for the resuspension factor, S_f , have emerged as a metric to predict the risk from inhaled radioactive particles. By taking the ratio of the volumetric airborne radioactivity to the ground deposited areal radioactivity, the resuspension factor can be directly measured.

$$S_f = \frac{\alpha_V A}{\alpha_A V} \quad (2)$$

In this equation α_V is the activity in the air, α_A is the activity on the surface, A is the area of the surface, and V is the volume being considered above the surface. This method gives S_f units of m^{-1} . Using this equation to measure the resuspension factor, scientists identified a nonlinear decay of the suspended particles over time. This is usually modeled as an exponential, but some models use polynomials or power-law

(Garger et al., 1999). These models are applied for prospective dose evaluation after the details of the contaminated area have been determined. However, when these models are used to predict the resuspension factor at early time frames ($t < 2 \text{ weeks}$) after deposition, the result is at least ten times more conservative than what is observed (Maxwell and Anspaugh, 2011).

The most prominent of these resuspension studies is the analysis by Maxwell and Anspaugh from 2011. This is the study from which the current resuspension factor model is taken. Maxwell and Anspaugh organized historical measurements of the resuspension factor from over sixty different studies into a single data set. Among these were several nuclear test sites, including the Schooner nuclear test site and the Simon test in the Upshot-Knothole Series. Data from reactor meltdowns, non-explosive plutonium test releases, and other sources were also included. The vast majority of these studies focused on airborne release events. Several of these studies took data points each week, often for years after release. The new, large dataset was fit with several different models until a double exponential model was settled on. This double exponential model is the currently accepted empirical model for predicting the resuspension factor.

The *FRMAC Assessment Manual* published by the Federal Radiological Monitoring and Assessment Center (FRMAC), determines the action limits in the event of a radiological incident (FRMAC, 2018). These limits are based on the same annual limits mentioned in section 2.1, and the analysis of resuspension conducted by Maxwell and Anspaugh in 2011. When calculating these limits for a contaminated area, each type of exposure pathway is considered separately. Inhalation is one of the considered exposure pathways, and the resuspension factor appears in the calculation of the

deposition inhalation dose parameter, D_{inh} (Sv). D_{inh} is the equivalent dose from inhaling suspended radionuclides, and can be calculated according to the following equation:

$$D_{inh} = C_{D,inh} \times \bar{f}_B \times KP \quad (3)$$

Where $C_{D,inh}$ is the inhalation committed dose coefficient for the radionuclide (Sv Bq⁻¹), and \bar{f}_B is the activity-averaged human breathing rate (usually 0.92 m³ h⁻¹). KP is the resuspension parameter (Bq s m⁻¹), which is a representation of the airborne concentration of the radionuclide over the given time. This parameter takes into account the the radioactive decay of the radionuclide, the resuspension factor $K(t)$, and the initial deposition of the radionuclide, D_p (Bq). KP can be calculated by:

$$KP = \int_{t_1}^{t_2} K(t) \times D_p \times e^{-\lambda t} dt \quad (4)$$

The current empirical resuspension factor is based on the work of Maxwell and Anspaugh (2011), and is given by the equation:

$$K(t) = (10^{-5})e^{-(8.1 \times 10^{-2})t} + (7 \times 10^{-9})e^{-(2.31 \times 10^{-3})t} + 10^{-9} \quad (5)$$

This predictive model will be compared to the measured data of this study.

2.4 Detection of Radionuclides

2.4.1 Neutron Activation Analysis

Neutrons are a type of ionizing radiation that can be absorbed into the nucleus of an atom and cause the atom to become unstable. The unstable atom will then usually

emit a photon when it decays. For many radionuclides, the energy of this photon is very specific. With a good detector, this energy can be used to identify specific elements and isotopes present in a sample. This process is called neutron activation analysis (NAA), and is a proven technique for the detection of trace quantities (Murrarka, 2006).

The process of NAA works by first activating a sample through exposure to neutrons. The activated sample is then placed in a detector. Figure 2 shows the process of a beta emitting nuclide returning to a stable state. The process of regaining stability releases a measurable gamma ray. Based on the energy readings of the detector, a mass of specific elements can be found.

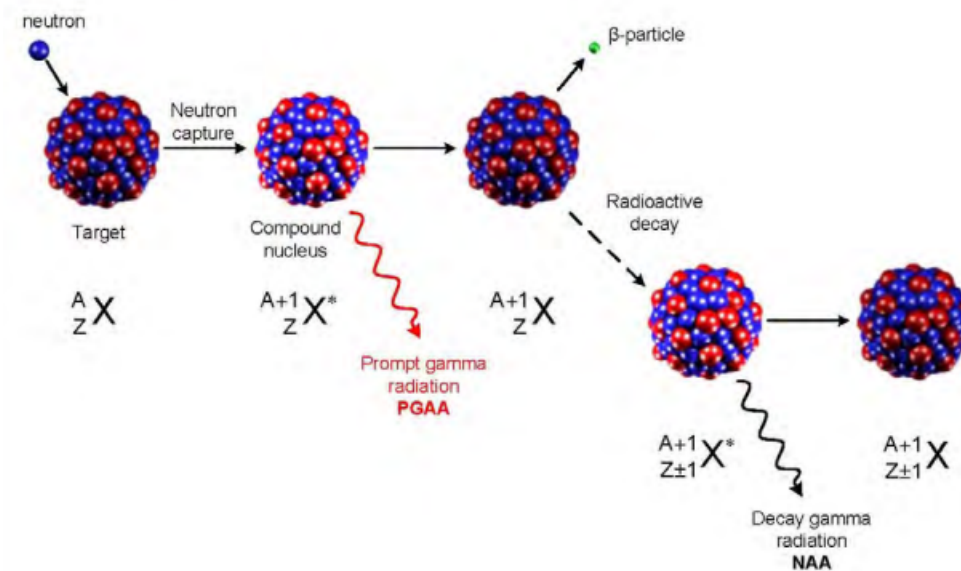


Figure 3: Diagram of how a neutron is absorbed by a nucleus and stimulates the emission of a gamma ray that can be measured by a detector for NAA (NMIII, 2012)

For example, when a neutron is absorbed by Europium (Eu) 153 it becomes Eu 154.

Eu 154 is an unstable isotope that decays by beta minus emission. In this process it will emit a 123.07 KeV photon with a 40% probability (Chu et al. 1999). The number of disintegrations in the sample can be found two ways, using either the counts from the detector or the mass of the sample. The number of disintegrations given by the mass of the sample is given by:

$$D_T = \sigma\phi N_T(1 - e^{-\lambda t}) \quad (6)$$

Where σ is the reaction probability, ϕ is the neutron flux (neutrons $\text{s}^{-2} \text{cm}^{-2}$), t is the irradiation time (s), and λ is the decay constant of the nuclide. N_T is the number of stable nuclides undergoing irradiation, which can be found via:

$$N_T = \left(\frac{m}{M}\right) X N_A \quad (7)$$

Where m is the mass of the desired sample, M is the molar mass of the isotope, X is the natural abundance of the isotope, and N_A is Avogadro's number. By combining these two equations and solving for the mass we obtain:

$$m = \frac{D_T M}{N_A X \sigma \phi (1 - e^{-\lambda t})} \quad (8)$$

The number of disintegrations D_T can be found from the counts given by the detector and the detector efficiency using the equation:

$$D_T = \frac{C}{\epsilon} \quad (9)$$

Where C is the number of counts from the detector and ϵ is the detector efficiency. This gives us a final equation for finding the mass of a given isotope via neutron

activation analysis:

$$m = \frac{CM}{\epsilon N_A X \sigma \phi (1 - e^{-\lambda t})} \quad (10)$$

2.4.2 Minimum detectable mass

This type of detection has its limits. A common measure of this limitation is the concept of a minimum detectable mass and an associated minimum detectable activity. This paper will follow the same derivation of minimum detectable mass as that found in Llyod Currie's *Limits for Qualitative Detection and Quantitative Determination* (1968). The minimum detectable activity can be determined by finding two quantities: The critical limit and the detection limit. A critical limit is a detected activity above which it is likely that there is radioactive material on the sample. This can be found by comparing the background count rate (C_b) and its associated uncertainty (σ_b) to the gross count rate (C_g) and its uncertainty (σ_g) and selecting a desired confidence level (k_α). This gives us an equation for the critical limit (after some simplification) as:

$$LC = k_\alpha \sqrt{2C_b} \quad (11)$$

The interpretation of this limit is that one may reject the null hypothesis when a gross count rate above LC is measured. This limit is prone to type II, or false negative, errors and is paired with another limit to take care of those types of error. This limit is known as the detection limit. The detection limit, which has its own confidence level (k_β), can be found using the critical limit via this equation:

$$LD = LC + \frac{k_\beta^2}{2} \left(1 + \sqrt{1 + \frac{4LC}{k_\beta^2} + \frac{4LC^2}{k_\alpha^2 k_\beta^2}} \right) \quad (12)$$

This detection limit is the limit above which it is likely for there to be radioactive material on the sample AND it is unlikely for there to be no radioactive material on the sample. For most purposes, the confidence levels k_α and k_β are the same (k). In this case, the equation for LD becomes:

$$LD = k^2 + 2LC = k^2 + 2k\sqrt{(2C_b)} \quad (13)$$

To determine our minimum detectable activity from our detection limit, we divide by our counting time (Δt) and our detector efficiency (ϵ) to finally get this equation for the minimum detectable activity:

$$MDA = \frac{k^2 + 2k\sqrt{(2C_b)}}{\epsilon\Delta t} \quad (14)$$

A minimum detectable mass is a related quantity that can be determined for the specific isotope that is being measured. By taking into account the production rate $P(\sigma)$ ($\frac{Bq}{g}$) of neutrons from the generator, the saturation $S(\lambda, \tau)$ of the sample, the time synchronization (τ) of the irradiation, the counting delay t , and the count we can write an expression for the minimum detectable mass:

$$MDM = \frac{L_D}{YP(\sigma)S(\lambda, \tau)T(\lambda, t, \Delta t)} \quad (15)$$

where in this equation

$$T(\lambda, t, \Delta t) = \left(\frac{e^{-\lambda t}}{\lambda}\right) \left(1 - e^{-\lambda\Delta t}\right), \quad (16)$$

$$S(\lambda, \tau) = 1 - e^{-\lambda\tau}, \quad (17)$$

$$P(\sigma) = \frac{N\sigma\phi}{m} \quad (18)$$

and λ is the decay constant, Y is the gamma yield for the isotope, m is the mass of the sample, and ϕ is the neutron flux. N is the quantity of activation product produced. This quantity can be obtained from the atomic weights and relative isotope abundance using the following formulas:

$$m = \sum \frac{M_{X_i} N_{X_i}}{N_A} = \frac{N_{X^*}}{N_A} \left(M_{X^*} + \sum_{i \neq *} \frac{M_{X_i} a_{X_i}}{a_{X^*}} \right) \quad (19)$$

$$N = N_{X^*} = \frac{m N_A}{\left(M_{X^*} + \sum_{i \neq *} \frac{M_{X_i} a_{X_i}}{a_{X^*}} \right)}$$

And thus the production rate, noted earlier as $P(\sigma)$ is defined as:

$$P(\sigma) = \frac{N_A \sigma \phi}{\left(M_{X^*} + \sum_{i \neq *} \frac{M_{X_i} a_{X_i}}{a_{X^*}} \right)} \quad (20)$$

Which finally allows us to obtain a complete expression for the minimum detectable mass of the system:

$$MDM = \frac{L_D \left(M_{X^*} + \sum_{i \neq *} \frac{M_{X_i} a_{X_i}}{a_{X^*}} \right)}{\epsilon Y N_A \sigma \phi (1 - e^{-\lambda t}) \left(\frac{e^{-\lambda t}}{\lambda} \right) (1 - e^{-\lambda \Delta t})} \quad (21)$$

2.4.3 Minimum Detectable Resuspension Factor

The resuspension factor, which this report seeks to determine, is dependent on the suspended mass and therefore a minimum detectable resuspension factor (MDS_f) also exists. The resuspension factor is the ratio of the volumetric concentration of mass in the air to the aerial deposition surface concentration, the minimum. The minimum detectable mass therefore finds its way into the numerator of this equation as a measure of the mass in the air. To make this a concentration we divide the MDM by the volume of air sampled and the efficiency of our detector. The volume of air sampled is directly proportional to the sampling rate f and the sampling time t_s . This gives us a numerator (g m^{-3}) for our minimum detectable resuspension factor of:

$$C_v = \frac{MDM}{\epsilon_F f t_s} \quad (22)$$

Our denominator is based on the ground deposited concentration of radioactive material. Therefore the denominator of our MDS_f is the initial deposition mass m_0 divided by the area of deposition A . Since our depositon mass often comes in the form of a compound, we include a factor of X_f , which is the fractional molecular mass of the isotope of interest in that compound. This gives us the concentration of the isotope of interest on the surface of interest, which we can write as:

$$C_s = \frac{m_0 X_f}{A} \quad (23)$$

Combining our numerator and denominator gives us MDS_f :

$$MDS_f = \frac{C_v}{C_s} = \frac{\frac{MDM}{\epsilon_F f t_s}}{\frac{m_0 X_f}{A}} \quad (24)$$

And inserting the expression for MDM and simplifying we obtain our final expression for the minimum detectable resuspension factor:

$$MDS_f = \frac{A(k^2 + 2k\sqrt{(2C_b)})\left(M_{X^*} + \sum_{i \neq *}\frac{M_{X_i}a_{X_i}}{a_{X^*}}\right)}{\epsilon Y m_0 N_A X_f f t_s \sigma \phi \epsilon_f (1 - e^{-\lambda t}) \left(\frac{e^{-\lambda t}}{\lambda}\right) (1 - e^{-\lambda \Delta t})} \quad (25)$$

3 Methods

3.1 Materials

3.1.1 Suspending Material

Europium oxide (Eu_2O_3 , $d_p > 1 \mu\text{m}$, Sigma-Aldrich Corp.) was chosen as the suspending material for several reasons. The first is that both of the natural isotopes of Europium (Eu), ^{151}Eu and ^{153}Eu are detectable by neutron activation analysis, as both ^{152}Eu and ^{154}Eu are unstable isotopes that can be created with NAA, and have gammas of greater than 10% probability. The second reason is that Eu is a chemical analog to Americium 241, which is a common contaminant released by reactors that work with plutonium.

3.1.2 Air Sampling

The air samplers used are low-volume vacuum pump air samplers (Atlantic Nuclear Corp.) which siphons at a flow rate of approx 2.0 L min^{-1} through a plastic nozzle fitted with a 47mm diameter carbon fiber filter (Hach co). The filter is stated by the manufacturer to have a 99% collection efficiency.

3.1.3 Resuspension chamber

The resuspension chamber is made up of a 6ft long acrylic tube with a 4.25 in (10.7cm) inner diameter (US Plastic Corp.). The inside of the tube was coated in soap before each experiment to help prevent particulates from sticking to the acrylic. The tube is open on both ends. The tube was stabilized by concrete blocks and straps (Home Depot Corp.). The stabilization prevents the chamber from breaking its seal while the air samplers are removed to collect and replace the filters.

3.1.4 Neutron Activation Analysis

Neutron activation analysis requires a *neutron source*, *gamma detector*, *gold foils*, slabs of *Solid Water*, and a healthy supply of *scotch tape*.

- **Neutron Source** The neutron source is an Adelphi Technology DD110M portable neutron generator which has a neutron flux of 10^7 n cm⁻² s⁻¹ at full power. Using Solid Water to scatter and thermalize fast neutrons back at the sample enhances the flux to 10^8 n cm⁻² s⁻¹ at full power (Marshall, 2021).
- **Gamma detector** The gamma detector is a High Purity Germanium detector. The detectors are regularly calibrated with check sources like Co-60, Mn-54, and Eu-152. Detector efficiency is calculated using the dating of the check sources.
- **Gold Foil** By activating a known mass of gold foil along with the sample, the neutron flux can be calculated each time a sample analysis is done.
- **Scotch Tape** Scotch tape is used to tape samples and gold foils to the front of the neutron generator.

3.2 Experiment setup

1. **Place deposition surface.** Ideally, the experiment should be conducted in an area with low traffic. This will reduce impact of resuspension by random vibrations. The deposition surfaces should be close to some shelving for the vacuum pumps to rest on. Place the deposition surface underneath and in front of the shelving.
2. **Stabilize the chambers.** Place concrete blocks and stabilization straps around the resuspension chamber so that the acrylic cannot move. The acrylic should stand on its own and be able to remain standing while removing air samplers to collect filters.
3. **Set up air samplers.** Connect the air sampler nozzle to the compressor and fit it with a filter.

3.3 Experiment Procedure

3.3.1 Collecting Samples

1. **Measure dispersal samples.** Use a digital scale and scooping utensils to weigh out a mass of europium oxide and place it into paper boats. Repeat this for each chamber constructed.
2. **Place sample onto deposition surface.** Measure out 5g of Eu_2O_3 . Gently lift the acrylic to place the Europium powder onto the deposition surface, then replace acrylic.
3. **For concrete or other hard surfaces.** Lift the base of the tube to one side and pour the sample into the chamber. Replace the acrylic tube, ensuring

that it completely surrounds the sample. Place stabilizers around the tube to reduce the movement of the tube.

4. **Begin sampling.** Lower the air sampler heads, with filters inside, into the resuspension chambers so that each head hangs .25m above the sample. Turn on the compressor; mark the start time. Lock the room and disallow public entry to prevent inadvertent air flow.
5. **Collect samples.** On an hourly, daily, or weekly basis, turn off the pumps and retrieve the air sampler filters. Sampler heads should be pulled gently out of the chambers so that the tube is not knocked around or vibrated. The filter is removed from the sampler head and placed into a sealed envelope. Replace the filters in each of the sampler heads and gently replace them into the chambers. Once all heads are returned to their chambers, turn the vacuum pumps back on and repeat these steps at the next time interval.
6. **Measure samples with NAA.** Once a sample has been obtained, the mass of Europium on the filter can be obtained using the process below.

Safety Measures

3.3.2 Neutron Activation Analysis

1. **Ramp up Generator.** The generator chamber must be evacuated to a near-vacuum state before usage. This requires running the roughing and turbo-pumps for at least 2-3 days before use. Turn on the chiller and high voltage power supply, and open the stop valve of the deuterium gas fuel. In the Lab-View computer interface, slowly increase the voltage of the magnetron and target chamber to their operating levels (5kV, 115mA for magnetron and 125kV

and 40mA for target). Voltage increases of about 15 kV at a time typically work well for ramping up the target. The process will take varying amounts of time depending on the amount of arcing and short circuits that are followed by a shutdown of the magnetron.

2. **Affix sample and gold foil to generator beam centerline** Tape a gold foil of known mass to a stack of envelopes containing filter samples. Then tape this to the centerline of generator beam at the front of the generator.
3. **Engage magnetron to begin irradiation.** With the magnetron voltage and current at their proper levels (125kV, 115mA), turn on the magnetron and irradiate for 8 hours. This is comparable to the 9.316 hour half-life of the prominent nuclear reaction $\text{Eu-151}(n,\gamma)\text{Eu-152m}$
4. **Halt irradiation, count foil activity.** Shut down the generator magnetron. Wait for a minute to allow the generator room to cool down, then bring the gold foil to HPGe detector, using tape as needed to secure the foil. Engage the high voltage on the detector and count the gamma events for 5-10 minutes.
5. **Count Sample Activity.** Place the gold foil into a shielded storage unit. Bring the sample to the HPGe detector, using tape as needed to secure the sample. Engage the high voltage on the detector and count the gamma events from the sample for 2-8 hours.

Safety Measures The primary safety concern for this section of the experiment is the absorbed dose from the neutron generator and the irradiated gold foil and samples. The occupational dose limits for adults (discussed in section 2.1) give an allowed yearly absorbed dose of 5 Rem or .05 Sv to the whole body.

While the Europium oxide powder is not naturally radioactive, both it and the gold foil become radioactive after neutron activation. There are three activated nuclides to consider, Eu 152, Eu 154, and Au 198. Following the analysis in (Marshall, 2020) the equivalent dose from an external gamma source for each of these nuclides can be estimated during transportation and counting. The gamma constants, the dose rate at a specified distance for a specified activity, are known for all three nuclides. Using the equation:

$$E = \frac{\Gamma A_0 t}{r^2} \quad (26)$$

We can calculate the equivalent dose of our sample by knowing the activity. Our activity can be calculated by

$$A = N\sigma\phi = \frac{mN_A\sigma\phi}{M} \quad (27)$$

We conservatively assume the gold has a mass of .1g and very conservatively assume there is .1g of Eu_2O_3 on the sample. Using the relative abundances of Eu-151 and Eu-153, and the relative masses of Europium and Oxygen, we obtain a mass of .0413g of Eu-151 and .0451 of Eu-153. Transportation takes approximately 2 minutes for both the sample and the gold. The gold is counted for 5-10 minutes, so we will assume 10 minutes. The Eu is counted for 2-8 hours, so we will assume 8 hours. We assume the gold and the sample are point sources 30cm away for transportation and point sources 50cm away during counting. From The total equivalent dose from all three sources, assuming maximum irradiation and counting time of 8 hours each, is 5.656×10^{-5} Rem. Assuming a technician performed this experiment each day for a year, this would only amount to .02 Rem/year (.021 in a leap year), which is well

within safety limits.

In order to limit exposure, the technician should maximize the distance between themselves and the active sources and minimize their time near sources. Other techniques, like shielding around areas where radioactive materials are counted, can further reduce exposure to radiation.

3.3.3 Calculation of the Resuspension Factor

Similar to the calculation of the minimum detectable resuspension factor. Using the counts from each sample, the resuspension factor can be calculated. Below is a table of all constants used to calculate the resuspension factor in this experiment with their values:

Parameter	Value	Description
k	1.645	k-value of 95% confidence of no Type-I or Type-II errors
Y_{Eu}	.1420	Average yield of 841.6KeV gammas from $^{151}Eu(n, \gamma)^{152}Eu$
Y_{Au}	.96	Average yield of 411.8KeV gammas from $^{197}Au(n, \gamma)^{198}Au$
σ_{Eu}	3.3×10^{-25}	(m^2) absorption cross section of $^{151}Eu(n, \gamma)^{152}Eu$
σ_{Au}	9.87×10^{-27}	(m^2) absorption cross section of $^{197}Au(n, \gamma)^{198}Au$
N_A	6.022×10^{23}	(mol^{-1}) Avogadro's number
M_{Eu-151}	150.9	($g mol^{-1}$) Molar mass of ^{151}Eu
M_{Eu-153}	152.9	($g mol^{-1}$) Molar mass of ^{153}Eu
M_{Au}	197.0	($g mol^{-1}$) Molar mass of ^{197}Au
a_{Eu-151}	0.4791	Relative abundance of ^{151}Eu
a_{Eu-153}	0.5219	Relative abundance of ^{153}Eu
λ	0.0746	(hr^{-1}) decay constant of ^{152}Eu
λ	0.0107	(hr^{-1}) decay constant of ^{198}Au
t_s	[1,24]	(hr) Air sampling time period
τ	2	(hr) Neutron irradiation time period
t	.13	(hr) Time delay between activation and gamma detection
Δt	2	(hr) Gamma detection time period
m_0	5.0	(g) Deposition mass
X_f	.7	Relative fraction of Eu to O in Eu_2O_3 by mass
A	9.152×10^{-3}	(m^2) Surface area of deposition
f	3.33×10^{-5}	($m^3 s^{-1}$) flow rate of air samplers
ϵ_F	0.99	Carbon fiber filter particulate capture efficiency
m_{Au}	Varies	(g) Mass of gold foil used for flux calibration
C^{Au}	Varies	Count of gamma events from Au foil
ϕ	Varies	(neutrons $cm^{-1} s^{-1}$) Neutron flux delivered to samples
C^*	Varies	Count of gamma events from irradiated sample

Table 1: List of values used in calculating the resuspension factor using the methods listed in this section.

These factors are used in the equations below to determine the resuspension factor and minimum detectable resuspension factor:

$$\phi = \frac{C^{Au} M_{Au}}{\epsilon Y_{Au} m_{Au} N_A \sigma_{Au} (1 - e^{-\lambda_{Au} \tau}) \left(\frac{e^{-\lambda_{Au} t}}{\lambda_{Au}} \right) (1 - e^{-\lambda_{Au} \Delta t})} \quad (28)$$

$$MDS_f = \frac{A(k^2 + 2k\sqrt{(2C_b)})\left(M_{X^*} + \sum_{i \neq *}\frac{M_{X_i}a_{X_i}}{a_{X^*}}\right)}{\epsilon Y m_0 N_A X_f f t_s \sigma \phi \epsilon_f (1 - e^{-\lambda t})\left(\frac{e^{-\lambda t}}{\lambda}\right)(1 - e^{-\lambda \Delta t})} \quad (29)$$

$$S_f = \frac{AC^*(M_{Eu-151} + \frac{M_{Eu-153}a_{Eu-153}a_{153}}{a_{Eu-151}})}{\epsilon_F Y_{Eu} m_0 X_F f t_s \epsilon N_A \sigma_{Eu} \phi (1 - e^{-\lambda_{Au} \tau})\left(\frac{e^{-\lambda_{Au} t}}{\lambda_{Au}}\right)(1 - e^{-\lambda_{Au} \Delta t})} \quad (30)$$

4 Results

Through neutron activation analysis and some calculations, the resuspension factor was determined for each resuspension chamber on each measured day. Each measured day was averaged to create a single point for each day with an associated uncertainty, obtained through the standard error of the mean. These average points are plotted below against the accepted resuspension factor model for small times. The fits applied to each data set are double exponential fits, similar to the Maxwell and Anspaugh fit. Each fit was determined by fixing the first exponential, then fitting the second exponential afterwards.

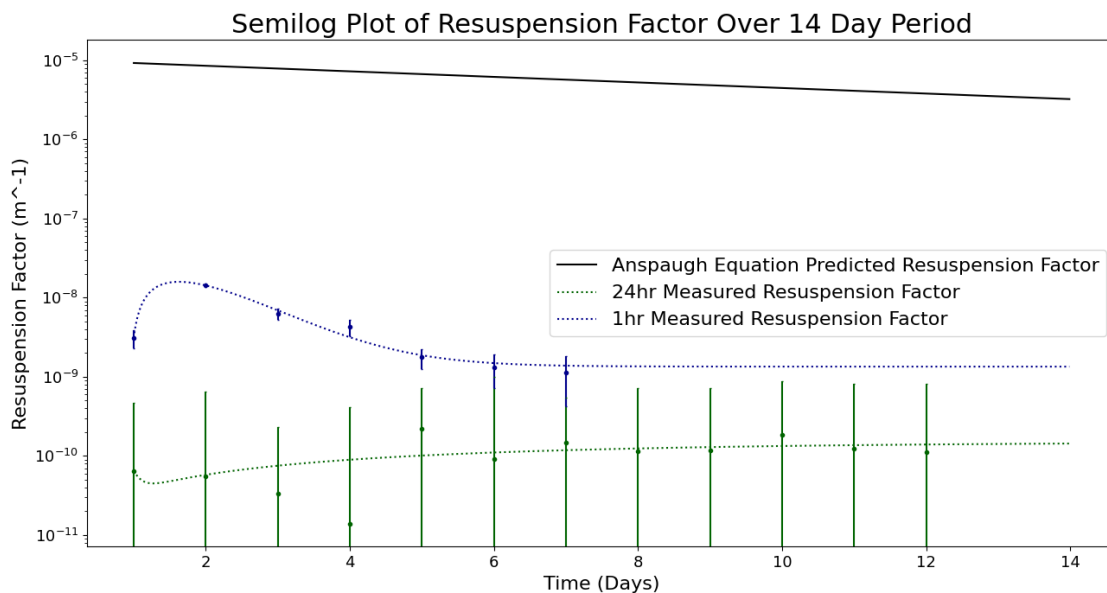


Figure 4: Semi-log of the average measured resuspension factor tests and the resuspension factor predicted by the Maxwell and Anspaugh resuspension factor equation for the first fourteen days after release.

Parameter	Maxwell and Anspaugh Fit	24 Hour Sampling	1 Hour Sampling
X_1	1.00E-04	-6.13E-08	1.02657851
X_2	7.00E-09	6.15E-08	-1.02657876
ω_1	-0.081	7.87E-01	1.52051846
ω_2	-0.00231	7.93E-01	1.52051872
b	1.00E-08	1.39E-10	1.34584E-09

Table 2: Fit parameters for the double exponential fits by Maxwell and Anspaugh, 24 hour air sampling, and 1 hour air sampling.

Day	Suspended Mass (Kg)	Minimum Detectable Sf (m-1)	Sf (m-1)
1	2.72E-16	2.04E-11	6.49E-11
2	2.33E-16	1.04E-11	5.56E-11
3	1.40E-16	6.06E-12	3.35E-11
4	5.85E-17	3.20E-12	1.40E-11
5	9.26E-16	1.26E-11	2.21E-10
6	3.85E-16	1.28E-11	9.20E-11
7	6.20E-16	5.12E-12	1.48E-10
8	4.79E-16	4.50E-12	1.14E-10
9	4.88E-16	4.16E-12	1.17E-10
10	7.79E-16	8.28E-12	1.86E-10
11	5.23E-16	5.77E-12	1.25E-10
12	4.65E-16	8.38E-12	1.11E-10

Table 3: Suspended mass, MDS_f , and S_f for a 24 hour sampling time. 24 hours was shown to oversample the chamber and led to a lower resuspension factor. For all samples, irradiation time was 2 hours, count time was 2 hours, transport time was .13 hours, and deposited mass was 5g.

Day	Suspended Mass (Kg)	Minimum Detectable Sf (m-1)	Sf (m-1)
1	1.30E-14	1.67E-09	3.10E-09
2	6.03E-14	1.27E-09	1.44E-08
3	2.62E-14	1.05E-09	6.26E-09
4	1.78E-14	1.67E-09	4.24E-09
5	7.36E-15	1.46E-09	1.76E-09
6	5.50E-15	1.12E-09	1.31E-09
7	4.69E-15	1.34E-09	1.12E-09

Table 4: Suspended mass, MDS_f , and S_f for a 1 hour sampling time, chosen after the 24 hour sampling was shown to oversample the resuspension chamber. For all samples, irradiation time was 2 hours, count time was 2 hours, transport time was .13 hours, and deposited mass was 5g. Data is cut short at seven days due to malfunction of the neutron generator, however samples past seven days were still collected. These samples will be evaluated once the neutron generator is repaired.

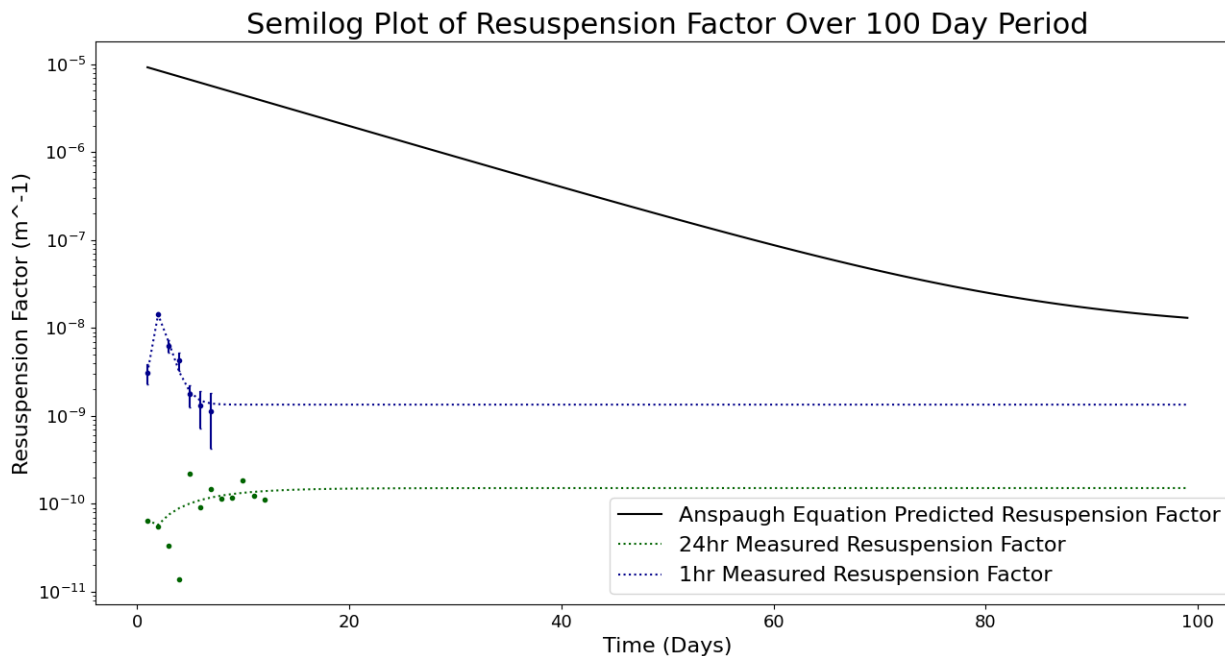


Figure 5: Semi-log of the measured resuspension factor tests and the resuspension factor predicted by the Maxwell and Anspaugh resuspension factor equation. Fits have been extended out to 100 days.

5 Analysis

5.1 Evaluation of Measured Resuspension Factor

Resuspension chambers were initially sampled for a 24 hour period. Later experiments changed this sampling period to one hour. Under the same conditions, the 24 hour sampled resuspension chambers yielded significantly smaller resuspension factors. 1 hour sampling always resulted in a resuspension factor at least one order of magnitude greater than 24 hour sampling. Even at the low flow rate 2L/m used in

this study, 24 hour sampling over-sampled the air in the resuspension chamber. All of the suspended mass accumulated on the filter at some time before 24 hours, leaving sampling time where nothing was collected. Consequently, the 1 hour sampling time of the resuspension factor should be considered a more accurate representation of the resuspension factor.

Due to malfunctions of the neutron generator used in neutron activation analysis, many samples were collected and unable to analyzed in this study. This includes the 1 hour samples past day seven in from Table 2. These samples will be analyzed at a later date when the neutron generator is operational again. Additionally, samples from varied surfaces and from aerial release scenarios were unable to be analyzed. These samples will also be properly analyzed when the neutron generator is repaired.

5.2 Evaluation of Predicted Resuspension Factor

The resuspension factor predicted by Maxwell and Anspaugh in the first twelve days is four or more orders of magnitude greater than the observed resuspension factor of any test. Typical observed variance in the resuspension factor is around two orders of magnitude (Maxwell and Anspaugh, 2011). Even providing all resuspension factors with this uncertainty, the predicted resuspension factor is still an overestimation.

For times greater than 50 days, the Maxwell and Anspaugh resuspension factor is within the 2 orders of magnitude variance that is expected for a difference in initial conditions.

There are several key differences between the data sets analyzed by Maxwell and

Anspaugh and this study. The historical data used by Maxwell and Anspaugh is often taken from nuclear testing sites and reactor meltdowns. These are uncontrolled environments with many more resuspending influences than the controlled setup of this study. Wind, precipitation, human and animal traffic, temperature, and other factors have been shown to have an affect on resuspension. Most of these influences have a positive correlation with resuspension. Since Maxwell and Anspaugh's resuspension model is based on studies where these influences are present, it will naturally overestimate any situation where these influences are removed. However, this on its own does not explain the four orders of magnitude gap between results. Tests on airborne release events in a controlled environment using the Maxwell and Anspaugh equation yielded a satisfactory approximation for other experiments (Marshall, 2021).

The historical data set also has many studies that survey the resuspension factor over very long periods of time. Data points that are a week or more apart are common, and leads to relatively few data points in the sensitive early times. Several data sets used by Maxwell and Anspaugh skip the first few weeks entirely, and measure the resuspension factor only once a month.

The final reason that could lead to this overestimation is the inclusion of initially suspended material in the measurement of the resuspension factor. The resuspension factor is calculated as the concentration of activity in the air divided by the areal deposition activity of the surface directly below it. This method of calculation makes no distinction between radioparticulates suspended during the initial release and radioparticulates resuspended at some time after the initial release. Since the historical data sets are taken from primarily airborne release events, the initially suspended particles are included in those measurements. Surface releases, as examined in this

study, will not have this initial suspension. This leads to an overestimation of the resuspension factor in the event of a surface release until such a time that the initially suspended particles have settled and only resuspended particles remain airborne. In the case of an airborne release, this effect will be more pronounced. After 50 days, the Maxwell and Anspaugh equation falls within the 2 order of magnitude expected variance. After 100 days, it falls within 1 order of magnitude and the slope of the curve levels out to match that of the measured fit. Once the initially suspended particles have all deposited and only resuspension is being measured, the predicted values and experimental values agree.

6 Conclusion

The generally accepted resuspension factor model is an overestimation of the resuspension factor at small times in the event of a surface release. The model could be improved by taking into account resuspending influences, collecting more data points for the model at small time frames, and accounting for the difference between an airborne release and a surface release. Making these corrections to the resuspension model is beyond the scope of this study, but is an excellent topic for further research. Specifically, it would be beneficial to develop a separate resuspension factor model for the event of a surface release. Further, it would be beneficial to acquire more data about the resuspension factor in early times, then refit the Maxwell and Anspaugh equation with this new data to improve accuracy.

Small time frames are a critical time for the resuspension factor to be accurately known. After several days or weeks, the contaminated area will often be evacuated and the resuspension factor would be needed to determine when the area is safe to

return to. At small times of just a couple days, individuals are still likely to be in the contaminated area. The resuspension factor is necessary to accurately evaluate the risk to these individuals. There are very few studies on the resuspension factor at these early times. More research is needed to ensure that the dose estimates given to these individuals are accurate.

Further research is needed to determine the conditions that affect resuspension in early time frames. In particular, the effect of deposition surface, precipitation, temperature, vibration, and particulate mass are as yet lightly studied or unstudied areas. A greater grasp on the factors that influence resuspension would allow for a new model to account for the conditions around a release to give a more accurate resuspension factor. Further research should also be conducted into the overestimation created by calculating the resuspension factor from an airborne release as opposed to a surface release.

The Maxwell and Anspaugh resuspension factor at small time frames does not accurately estimate the resuspension factor for surface releases. The model does accurately estimate surface releases and airborne releases at large times. However, small times are the most likely time for an individual to be in a contaminated area. Further work must be done to update the Maxwell and Anspaugh equation to more accurately assess the risk to individuals within contaminated areas.

References

- [1] Center for Disease Control. Acute Radiation Syndrome. *CDC.gov*, 2021.
- [2] L.A. Currie. Limits for qualitative detection and quantitative determination. *Analytical Chemistry*, 40:586–593, 1968.
- [3] M. Dreicer, T.E. Hakonson, C.G. White, and F.W. Whicker. Rainsplash as a mechanism for soil contamination of plant surfaces. *Health Physics*, 46(1):177–187, 1984
- [4] FRMAC. FRMAC assessment manual, volume 1, overview and methods. Sandia Report SAND2015-2884R, Federal Radiological Monitoring and Assessment Center, Albuquerque, NM, Apr. 2018.
- [5] E.K. Garger, F.O. Hoffman, K.M. Thiessen, D. Galeriu, A.I. Kryshev, T. Lev, C.W. Miller, S.K. Nair, N. Talerko, and B. Watkins. Test of existing mathematical models for atmospheric resuspension of radionuclides. *Journal of Environmental Radioactivity*, 42:157–175, 1999.
- [6] E.K. Garger, V. Kashpur, G. Belov, V. Demchuk, J. Tschiersch, F. Wagenpfeil, H.G. Paretzke, F. Besnus, W. Hollander, J. Martinez-Serrano, and I. Vintersved. Measurement of resuspended aerosol in the chernobyl area i. discussion of instrumentation and estimation of measurement uncertainty. *Radiation Environmental Biophysics*, 1997.
- [7] A.R. Harris and C.I. Davidson. Particle resuspension in turbulent flow: A stochastic model for individual soil grains. *Aerosol Science and Technology*, 42:613–628, 2008.

- [8] ICRP. Human respiratory tract model for radiological protection. *ICRP Publication 66*, 1994.
- [9] ICRP. Individual monitoring for internal exposure of workers. *IRCP Publication 78*, 1997.
- [10] E. Karlsson, I. Fangmark, and T. Berglund. Resuspension of an indoor aerosol. *Journal of Aerosol Science*, 27(Supplement 1):S441–S442, 1996.
- [11] Y. Kim, G. Wellum, K. Mello, K.E. Strawhecker, R. Thoms, A. Giaya, and B.E. Wyslouzild. Effects of relative humidity and particle and surface properties on particle resuspension rates. *Aerosol Science and Technology*, 50(4):339–352, 2016.
- [12] W.H. Langham. Plutonium distribution as a problem in environmental science. *Proceedings of Environmental Plutonium Symposium*, LA-4756:3–11, 1971
- [13] M.S. Lee and C.W. Lee. Association of fallout-derived cs-137, sr-90 and pu-239, pu-240 with natural organic substances in soils. *Journal of Environmental Radioactivity*, 47: 25362, 2000.
- [14] NCRP. Recommended screening limits for contaminated surface soil and review of factors relevant to site-specific studies. *Technical Report 129, National Council on Radiation Protection and Measurements*, 1999.
- [15] NMIII. Neutron capture. <http://nmi3.eu/neutron-research/techniques-for-chemicalanalysis.html>, 2012. [Image]. Accessed: 2022-04-20.
- [16] S.A. Marshall. Environmental Resuspension and Health Impacts of Radioactive Particulate Matter. *Worcester Polytechnic Institute*, 2021.

- [17] R.M. Maxwell and L.R. Anspaugh. An improved model for prediction of resuspension. *Health Physics*, 101(6):722–730, 2011.
- [18] Z. Xu, T. Jordan, and W. Breitung. Particle resuspension model for subatmospheric conditions. *IEEE Transactions on Plasma Science*, 44(9):1662–1665, 2016.